DR SHUICHI OKAMOTO (Orcid ID : 0000-0002-2751-4904)

DR SHOGO TAMURA (Orcid ID : 0000-0002-4960-1400)

DR ATSUO SUZUKI (Orcid ID : 0000-0002-7194-3183)

PROF. TETSUHITO KOJIMA (Orcid ID : 0000-0002-1905-1065)

DR NOBUAKI SUZUKI (Orcid ID : 0000-0003-2250-7964)

Article type : Original Article

Title

VWF-Gly2752Ser, a novel non-cysteine substitution variant in the CK domain, exhibits severe secretory impairment by hampering C-terminal dimer formation

Author names

Shuichi Okamoto *, Shogo Tamura ‡, Naomi Sanda §, Koya Odaira ‡, Yuri Hayakawa ‡, Masato Mukaide ‡, Atsuo Suzuki §, Takeshi Kanematsu ¶, Fumihiko Hayakawa ‡, Akira Katsumi **, Hitoshi Kiyoi *, Tetsuhito Kojima ‡ #, Tadashi Matsushita † ¶, Nobuaki Suzuki †

Author's affiliations

This article has been accepted for publication and undergone full peer review but has not been through the copyediting, typesetting, pagination and proofreading process, which may lead to differences between this version and the Version of Record. Please cite this article as doi: 10.1111/JTH.15746

* Department of Hematology and Oncology, Nagoya University Graduate School of Medicine, Nagoya, Japan

† Department of Transfusion Medicine, Nagoya University Hospital, Nagoya, Japan

‡ Division of Cellular and Genetic Sciences, Department of Integrated Health Sciences, Nagoya University Graduate School of Medicine, Nagoya, Japan

§ Department of Medical Technique, Nagoya University Hospital, Nagoya, Japan

¶ Department of Laboratory Medicine, Nagoya University Hospital, Nagoya, Japan

** Department of Hematology, National Center for Geriatrics and Gerontology, Obu City, Japan

Aichi Health Promotion Foundation, Nagoya, Japan

Corresponding author's contact information

Nobuaki Suzuki, M.D., Ph.D.

Department of Transfusion Medicine, Nagoya University Hospital

65 Tsurumai-cho, Showa-ku, Nagoya, Aichi 466-8560, Japan

Tel: +81-52-744-2652; Fax: +81-52-744-2610

Email: suzukin@med.nagoya-u.ac.jp

Running head

The VWF-Gly2752Ser variant causes type 3 VWD

ESSENTIALS

- A type 3 VWD-associated non-cysteine substitution in the CK domain has not been reported.
- *VWF* c.8254 G>A (VWF-Gly2752Ser) is a novel non-cysteine missense variation in the CK domain.
- VWF-Gly2752Ser causes dimerization failure, resulting in abnormal ER retention.
- VWF-Gly2752Ser is a deleterious variant causing type 3 VWD by its severe secretory impairment.

SUMMARY

Background: Von Willebrand factor (VWF) is a multimeric glycoprotein that plays important roles in hemostasis and thrombosis. C-terminal interchain-disulfide bonds in the cystine knot (CK) domain are essential for VWF dimerization. Previous studies have reported that missense variants of cysteine in the CK domain disrupt the intrachain-disulfide bond and cause type 3 von Willebrand disease (VWD). However, type 3 VWD-associated non-cysteine substitution variants in the CK domain have not been reported.

Objective: To investigate the molecular mechanism of a novel non-cysteine variant in the CK domain, *VWF* c.8254 G>A (p.Gly2752Ser), which was identified in a patient with type 3 VWD as homozygous.

Methods: Genetic analysis was performed by whole exome sequencing and Sanger sequencing. VWF multimer analysis was performed using SDS-agarose electrophoresis. VWF production and subcellular localization were analyzed using *ex vivo* endothelial colony forming cells (ECFCs) and an *in vitro* recombinant VWF (rVWF) expression system.

Results: The patient was homozygous for VWF-Gly2752Ser. Plasma VWF ELISA showed that the VWF antigen level of the patient was 1.2% as compared to healthy subjects. A tiny amount of VWF was identified in the patient's ECFC. Multimer analysis revealed that the circulating VWF-Gly2752Ser presented only low-molecular weight multimers. Subcellular localization analysis of VWF-Gly2752Ser-transfected cell lines showed that rVWF-Gly2752Ser was severely impaired in its ER-to-Golgi trafficking.

Conclusion: VWF-Gly2752Ser causes severe secretory impairment due to its dimerization failure. This is the first report of a *VWF* variant with a non-cysteine substitution in the CK domain that causes type 3 VWD.

KEYWORDS

Blood Coagulation Factors

Mutation, Missense

Protein Multimerization

von Willebrand Factor

von Willebrand Diseases

INTRODUCTION

Von Willebrand factor (VWF) is a large glycoprotein (>250 kDa), mainly synthesized in vascular endothelial cells, which plays a role in platelet adhesion to subendothelial tissues and as a carrier protein of coagulation factor VIII (FVIII) [1, 2]. In the process of VWF production, VWF monomers (VWF subunits) are dimerized via interchain-disulfide bonds between the C-terminal cystine knot (CK) domains [3-6]. The dimerized VWFs are further joined with intermolecular-disulfide bonds from the N-terminal D´ D3 domain [7, 8], which results in a large string structure, called a high molecular weight multimer (HMWM), of over 20,000 kDa [1]. The HMWMs are secreted into circulating blood or stored in Weibel-Palade bodies (WPBs) within vascular endothelial cells [1, 2, 8, 9]. The HMWM is a functional structure for physiological platelet aggregation (primary hemostatic plug formation). However, unusually large molecular weight multimers (ULMWMs) cause excessive platelet aggregation in vessels, resulting in thrombotic thrombocytopenic purpura (TTP) [10, 11]. To prevent the generation of ULMWM of VWF, A Disintegrin-like and Metalloproteinase with Thrombospondin type I motifs 13 (ADAMTS13) regulates the size of the VWF multimer by cleavage of the VWF A2 domain [12-14].

Von Willebrand disease (VWD) is a congenital bleeding disorder caused by qualitative or quantitative abnormalities of VWF due to *VWF* gene variations. VWD is classified into three major groups according to its etiology [15]. Type 1 VWD is a quantitative deficiency of VWF, and type 2 VWD is a qualitative deficiency. Type 2 VWD is subcategorized to type 2A (decreased VWF-dependent platelet adhesion with selective deficiency of HMWMs), 2B (increased affinity for platelet glycoprotein Ib), 2N (markedly decreased binding affinity for FVIII), and 2M (decreased VWF-dependent platelet adhesion without selective deficiency of HMWMs) based on the disease-associated molecular characteristics [15]. Type 2A VWD is further subdivided into

type 2A group I (impairment of VWF intracellular transport) and group II (increased sensitivity to ADAMTS13) [15, 16]. Type 3 VWD is a virtually complete deficiency of VWF, which is caused by genetic variations with a null phenotype (e.g., nonsense variations, frameshifts, or splice site variations) in most cases [15].

At the molecular level, it has been reported that type 3 VWD [15, 17-20] is in several cases caused by intracellular dimerization failure of VWF subunits. In particular, genetic missense variations associated with a cysteine substitution in the CK domain cause type 3 VWD resulting from intracellular dimerization failure (e.g., VWF Cys2739Tyr [18-20] and Cys2754Trp [17-20]). The disruption of inter- or intrachain-disulfide bond(s) within the CK domain severely impairs its intracellular transportation and extracellular secretion [5, 17-20]. However, type 3 VWD with a non-cysteine missense variation in the CK domain and its disease-associated molecular basis has never been reported.

In this study, a Japanese male patient with type 3 VWD was genotyped, and a novel single base substitution, *VWF* c.8254 G>A (p.Gly2752Ser), was identified as being homozygous. VWF-Gly2752Ser is a non-cysteine missense variation in the CK domain. To clarify the mechanism by which VWF-Gly2752Ser causes type 3 VWD, we investigated its molecular characteristics.

MATERIALS AND METHODS

Patient and samples

The patient is a 49-year-old Japanese male with the type 3 VWD phenotype. The patient's clinical data and bleeding episodes are described in the Results section. After obtaining written informed consent, blood samples were collected from the patient and his relatives (Figure 1A). Citrated plasma was subjected to hematological evaluation and experiments as described below. Genomic DNA was extracted from leukocytes in peripheral blood. For this study, we obtained ethical approval from the Ethics Review Committee of Nagoya University Graduate School of Medicine (identification number: 2015-0391, 2016-0477).

Genetic analysis

Whole exome sequencing (WES) was performed by a laboratory (Hokkaido System Science, Japan). Sequencing libraries were prepared using the SureSelect XT Human All Exon V5+UTRs Kit (Agilent Technologies, Santa Clara, California, USA) following the manufacturer's instructions. The libraries were sequenced on the HiSeq (Illumina, San Diego, California, USA) 2500 sequencing platform using HiSeq SBS Kit v4 reagents with 2 × 101 cycles. The adapter sequences and low-quality regions were trimmed by Cutadapt and Trimmomatic, respectively. After pre-processing, the reads were mapped to human reference genome GRCh37 (hg19) using BWA-0.7.10. Local realignment around known indels was performed by GATK-Lite-2.3.0 on the sorted BAM files, and Picardtools-1.115 was used to remove PCR duplicates. Finally, base quality score recalibration was performed using GATK again. Samtools-mpileup [options: -d 10000 -L 10000 -B -t DP, DV, SP, DP4, DPR] was piped with bcftools call [options: -A -v -m -f GQ] to produce VCF files.

Sanger sequencing was performed to confirm the *VWF* variant identified by WES. *VWF* exon 52, including 5′ and 3′exon-intron boundaries of *VWF*, was amplified by polymerase chain reaction (PCR) using KOD FX DNA polymerase (Toyobo, Osaka, Japan) and gene-specific primers (Supplementary Table 1). The PCR product was separated by 1.5% agarose gel electrophoresis and purified using a FastGene Gel/PCR Extraction kit (Nippon Genetics, Tokyo, Japan). Direct sequencing was performed using the BigDye™ Terminator v1.1 Cycle Sequencing Kit and ABI Prism 3130 Genetic Analyzer (Applied Biosystems, Waltham, Massachusetts, USA). Genetic variation is described according to the Human Genomic Variation Society (HGVS) nomenclature.

Measurement of VWF antigen and activity

Measurement of VWF antigen (VWF:Ag), ristocetin co-factor activity (VWF:RCo), and Factor VIII activity (FVIII:C) were outsourced to SRL (Tokyo, Japan). VWF:Ag was assayed by the latex agglutination method, and VWF:RCo was by the fixed platelet agglutination method. FVIII:C was measured by the coagulation time method. VWF:Ag in plasma and cell culture samples (shown below) was also measured by our in-house enzyme linked immunosorbent assay (ELISA) according to the protocol established by the World Federation of Hemophilia [21]. The detailed protocol of ELISA is described in the supplementary information.

Establishment of endothelial colony forming cells (ECFC)

We established ECFC in accordance with a previous publication [22]. Healthy control ECFCs were isolated from a healthy donor who did not have any hematological abnormalities. We obtained approximately 60 mL of blood from the forearm vein by a syringe with 1000 U of

heparin sodium (Mochida Pharmaceutical, Tokyo, Japan). The blood was stratified onto Ficoll-paque™ (GE Healthcare, Illinois, Chicago, USA) and centrifuged at 400 *g* for 35 min, followed by collecting the buffy coat. As a washing step, cells were diluted 1:1 with PBS and centrifuged at 300 *g* for 15 min. The cell pellet was resuspended in Endothelial Growth Medium-2 (EGM-2, Promo Cell, Heidelberg, Germany) supplemented with 0.2 μg/mL hydrocortisone, 10 ng/mL rhbFGF, 0.5 ng/mL vascular endothelial growth factor (VEGF), 20 ng/mL R3-IGF-1, 5 ng/mL rhEGF, 1 μg/mL ascorbic acid, 22.5 μg/mL heparin, and 0.1% GA-1000 (LONZA, Basel, Switzerland). Cells were seeded onto type I collagen-coated 6-well plates (Corning, One Riverfront Plaza, New York, USA) and cultured at 37 °C, 5% CO_2 and 95% humidity.

VWF multimer analysis and SDS-PAGE/WB

Multimer analysis was performed by SDS-agarose gel electrophoresis according to the protocol established by the World Federation of Hemophilia [21]. The detailed protocols of these analyses are described in the supplementary information.

Overexpression experiments of recombinant VWF (rVWF)

rVWF was overexpressed according to our previous publication [23]. In brief, plasmid pSVHVWF1.1 [24] is a wild-type (WT) rVWF-expressing vector that contains a full-length normal human VWF coding sequence inserted into the pSV7D plasmid [25]. The VWF-Gly2752Ser variant-expressing vector, pSVHG2752S, possesses a G-to-A transition at nucleotide 8,254 of pSVHVWF1.1, resulting in a substitution of glycine with serine at amino acid 2,752 of mature VWF. pSVHG2752S was generated by site-directed mutagenesis with specific primers (Supplementary Table 1).

COS-7 cells and HEK293 cells were cultured in Dulbecco's modified Eagle's medium (DMEM) supplemented with L-glutamine, phenol red (Sigma-Aldrich, St. Louis, Missouri, USA), and 10% (v/v) fetal bovine serum (Sigma-Aldrich) at 37 °C in 5% CO_2. The rVWF-expressing vector, pSVHVWF1.1 or pSVHG2752S, was transiently transfected into the cells using lipofectamine® 3000 (Thermo Fisher Scientific, Waltham, Massachusetts, USA) following the manufacturer's instructions. At 24 h post-transfection, the cells were washed once with PBS and cultured with

serum-free DMEM. At 72 h after transfection, the transfected cell culture media was harvested. The culture media was centrifuged at 15,200 *g* for 5 min at 4 °C. For VWF multimer analysis, collected culture media was concentrated by Amicon Ultra-100K (Merck, Darmstadt, Germany). The transfected cells were collected by centrifugation at 430 *g* for 5 min at room temperature. The pellet was temporarily preserved at –80 °C until analysis. The frozen pellet was lysed with lysis buffer (1% NP-40, 150 mM NaCl, 50 mM Tris, PMSF 1 mM, pH 8.0) and incubated on ice for 15 min, followed by centrifugation at 15,200 *g* for 5 min at 4 °C. The supernatant was collected as a cell lysate and cryopreserved at -80 °C until analysis.

Immunocytochemistry of VWF

Intracellular VWF in ECFC or rVWF-transfected cells were evaluated by immunofluorescence staining. We used mouse anti-human VWF antibody (M0616, DAKO, Carpinteria, California, USA) as the primary antibody and goat anti-mouse IgG (H+L) Alexa Fluor®488 or Alexa Fluor®555 conjugate as the secondary antibody (Thermo Fisher Scientific). VE-cadherin was detected by an anti-VE- cadherin antibody (ab33168, Abcam, Cambridge, UK) as the primary antibody and goat anti-rabbit IgG (H+L) Alexa Fluor®594 conjugate as the secondary antibody (Thermo Fisher Scientific). For intracellular sub-localization analysis, rVWF

was co-stained with the endoplasmic reticulum (ER) or Golgi apparatus. ER was stained with Protein Disulfide Isomerase (PDI) polyclonal antibody (Proteintech, Chicago, Illinois, USA) as the primary antibody and goat anti-rabbit IgG (H+L) Alexa Fluor®594 conjugate as the secondary antibody (Thermo Fisher Scientific). The Golgi apparatus was stained with Lectin-HPA Alexa Fluor®488 conjugates (Invitrogen, Carlsbad, California, USA). Nuclei were stained by 4'-6-diamino-2-phenylindole (DAPI) (Vector Laboratories, Burlingame, California, USA). Immunostained samples were observed by a confocal microscope, A1Rsi (Nikon, Tokyo, Japan) with Plan Apo Lambda 100×/1.45 oil immersion objective, image size of 512px × 512px and laser intensity fixed at 5.0% in all channels. rVWF co-localization with the ER or Golgi apparatus was statistically evaluated by Pearson's correlation coefficient (PCC) score using ImageJ Fiji's plugin, Coloc2 (https://imagej.net/Coloc_2). The PCC score was estimated from at least 10 cells for each rVWF.

Statistics

Quantitative data are described as mean ± standard error of the mean (SEM) values. Statistical analyses were carried out using IBM®SPSS®version 27 (International Business Machines corporation, Armonk, New York, USA). Comparisons of mean value and multiple groups were performed by Student's *t* test and one-way analysis of variance (one-way ANOVA) with Tukey's honestly significant difference test, respectively.

RESULTS

Patient's clinical presentation and molecular phenotyping

The patient has suffered from recurrent, lengthy nasal bleeding, but there have been no bleeding episodes in his relatives (Figure 1A). Although he has not received prophylactic clotting factor replacement therapy, he has never had any critical bleeding episodes. In the ISTH-SSC Bleeding Assessment Tool [26], the proband has a score of 8 points based on his epistaxis and bleeding from minor wounds. In the laboratory data, the levels of VWF:RCo were under the minimum detection sensitivity (6%), whereas his FVIII:C was 11% (Table 1). Genetic analysis by WES and Sanger sequencing identified a novel single base substitution at *VWF* exon 52, c.8254 G>A, which corresponds to an amino acid substitution at position 2,752 of a glycine with a serine, Gly2752Ser (Figure 1B). Genotyping analysis indicated that the patient carries this variation as homozygote, and his parents (who are cousins) and sons are heterozygotes (Figure 1A). Heterozygous individuals did not have any symptoms, suggesting that VWF-Gly2752Ser has an autosomal recessive inheritance pattern. To evaluate the pathogenicity of the VWF-Gly2752Ser variant, we performed *in silico* analyses by calculating the combined annotation dependent depletion (CADD) [27, 28] and Grantham scores [29]. The CADD and Grantham scores of the Gly2752Ser variant were 32 and 56, respectively. These data suggested that the Gly2752Ser variant is a significant pathogenic variant with regard to VWF function.

To further assess the patient's phenotype at the molecular level, we established an in-house VWF:Ag ELISA and subsequently investigated the VWF structure by multimer analysis and non-reducing SDS-PAGE/WB (Figure 1C and D). The VWF ELISA showed that the patient's plasma VWF:Ag level was 0.12 μg/mL (Table 1), which is approximately 1.2% of that of normal

pooled plasma (100% of VWF:Ag is defined as 10 μg/mL [30], and the normal range is generally 50–200% [31]). The VWF:RCo and VWF:Ag levels of the patient's parents (over 80 years of age) were more than 130% each, but the VWF:RCo levels of the patient' s 13-year-old and 11-year-old sons were mildly reduced to 79% and 42%, respectively. There were no blood type O individuals in the family, which has been reported to have decreased VWF plasma levels [32].

VWF multimer analysis showed that the proband's plasma contained trace amounts of the lowest molecular weight VWF, and those larger than dimeric molecular weight forms were absent (Figure 1C). However, the patient had a slower or faster migrating satellite band, suggesting there are trace levels of higher and lower-sized assemblies of VWF subunits. Non-reducing SDS-PAGE/WB showed that the patient's VWF had an approximately 500 kDa band (Figure 1D), indicating that quite a low amount of VWF-Gly2752Ser formed molecules of which the size corresponded to two VWF subunits and circulated. Regarding the patient's family members who are heterozygotes of VWF-Gly2752Ser, we could not examine their VWF molecular characteristics, because their blood samples were not available.

Analysis of VWF processing as visualized by ECFCs established from the patient's peripheral blood mononuclear cells (PBMCs)

To investigate the production of VWF-Gly2752Ser in vascular endothelial cells, we established *ex vivo* ECFCs derived from the patient's PBMCs and examined their VWF production. ECFC colonies generally emerged at 14–21 days after culture onset [33, 34]. In our case, ECFC colonies with cobblestone morphology (Figure 2A) were detected from culture days 10 to 26 after the seeding of fractionated PBMCs, and the mean culture day was day 15 ± 1. In immunostaining analysis, rod-shaped WPBs (a VWF signal) were observed entirely within the

cytoplasm of ECFCs derived from a healthy individual, whereas in the patient-derived ECFCs, small WPBs were observed at the perinuclear space (Figure 2B). These results suggest that the production and/or secretion of VWF-Gly2752Ser is severely impaired in vascular endothelial cells, which is consistent with the circulating VWF levels in the patient's plasma.

Recombinant expression and molecular characteristics of VWF-Gly2752Ser

Given that VWF-Gly2752Ser resulted in intracellular production and/or secretion failure, we further investigated the molecular pathogenesis of VWF-Gly2752Ser using a recombinant VWF (rVWF) overexpression system. Using the rVWF-WT expression vector pSVHVWF1.1 [24], we generated a rVWF-Gly2752Ser expression vector, pSVHG2752S, by site-directed mutagenesis. We transfected these vectors into COS-7 cells and quantitatively evaluated the amounts of rVWF in the culture media and cell lysate. In the culture media, the amounts of rVWF-WT and rVWF-Gly2752Ser were 0.126 ± 0.003 μg/mL and 0.020 ± 0.004 μg/mL, respectively. The extracellular secretion of rVWF-Gly2752Ser was significantly decreased to 15.5 ± 3.3% that of rVWF-WT (Figure 3A, medium). In the cell lysate, the amounts of rVWF-WT and rVWF-Gly2752Ser were 1.023 ± 0.050 μg/mL and 1.129 ± 0.032 μg/mL, respectively. The intracellular amount of rVWF-Gly2752Ser was 110.3 ± 3.2% that of rVWF-WT (Figure 3A, lysate). These results indicate that rVWF-Gly2752Ser shows secretion failure, consistent with the patient's phenotype.

We next investigated the multimeric structure of rVWF-Gly2752Ser. In multimer analysis of secreted rVWF in the culture media, rVWF-WT showed a typical multimeric pattern. rVWF-Gly2752Ser was mainly detected as a dimerized molecule (Figure 3B, medium). In addition, rVWF-Gly2752Ser with a size of four VWF subunits (tetramer) was slightly secreted into the medium (Figure 3B, open arrowhead). In the cell lysate, almost all rVWF-Gly2752Ser

was detected as the size of a VWF subunit (monomer). In addition, there was a trace amount of rVWF-Gly2752Ser of two subunits in size in the cell lysate (dimer, Figure 3B, lysate). Non-reducing SDS-PAGE/WB showed that although there was an abundant amount of rVWF-Gly2752Ser of monomer size, the form with two rVWF-Gly2752Ser subunits was also detected in both the extracellular and intracellular samples (Figure 3C). These observations suggest that rVWF-Gly2752Ser results in impaired dimer formation intracellularly, but small amounts of rVWF-Gly2752Ser subunits were intracellularly linked pairwise and transported into the medium.

VWF multimerization is formed by N-terminal interchain disulfide bonds of Cys1099-1099′ and Cys1142-1142′ in the D′D3 domain [7]. To rule out the possibility that VWF-Gly2752Ser dimers were formed by N-terminal interchain disulfide bonds, we generated the variants rVWFs, rVWF-Cys1099Ala/Cys1142Ala, and rVWF-Cys1099Ala/Cys1142Ala/Gly2752Ser and investigated their molecular characteristics by multimer analysis (Supplementary Figure 1). The multimer analysis showed that rVWF-Cys1099Ala/Cys1142Ala was detected as a dimer form that interlinked via only C-terminal disulfide bonds. In rVWF-Cys1099Ala/Cys1142Ala/Gly2752Ser, the variant rVWF molecules were detected as dimers and monomers, which is consistent with the multimer pattern of rVWF-Gly2752Ser. These observations suggest that limited VWF-Gly2752Ser dimerization is mediated through the C-terminal CK domains.

rVWF-Gly2752Ser displays intracellular trafficking failure

To further investigate the secretory impairment of rVWF-Gly2752Ser, we transfected rVWF-WT and Gly2752Ser expression vectors into HEK293 cells and analyzed the subcellular

localization of rVWF-Gly2752Ser to the ER or Golgi apparatus**.** We immuno-stained PDI as a marker of the ER [35-37]. By co-staining of rVWF and the ER, the rVWF-Gly2752Ser signal was thoroughly overlaid with the ER marker (Figure 4A). In the co-staining of rVWF and the ER with PDI, the PCC score of rVWF-Gly2752Ser was significantly higher than that of rVWF-WT (0.55 ± 0.02 vs 0.22 ± 0.05, $P < 0.001$) (Figure 4B). By co-staining of rVWF and the Golgi apparatus with Lectin-HPA (Figure 4C), the PCC score of rVWF-Gly2752Ser was significantly lower when compared to that of rVWF-WT (0.20 ± 0.04 vs 0.48 ± 0.03, $P < 0.001$) (Figure 4D). These results suggest that rVWF-Gly2752Ser causes abnormal ER retention because of a severe impairment in ER-to-Golgi trafficking.

rVWF-Gly2752Ser weakly suppresses rVWF-WT multimer formation in a dominant-negative manner

We also examined whether rVWF-Gly2752Ser can inhibit the multimer formation and/or secretion of rVWF-WT in a dominant-negative manner as seen in many type 1 VWD patients. For this purpose, rVWF-WT and Gly2752Ser expression vectors were co-transfected into COS-7 cells in various ratios (Figure 5A). Multimer analysis of the culture media showed that the large size multimers of rVWF-WT disappeared in a dose-dependent manner when rVWF-Gly2752Ser was added (Figure 5B, medium). In the cell lysate, the dimer formation of rVWF-WT was suppressed, and monomeric VWF molecules were increasingly detected in a dose-dependent manner with the addition of rVWF-Gly2752Ser (Figure 5B, lysate). Furthermore, a quantitative rVWF:Ag assay by ELISA showed that the extracellularly secreted rVWF was significantly reduced in a dose-dependent manner with the addition of rVWF-Gly2752Ser (Figure 5C, medium). In contrast, the intracellular rVWF level was increased with rVWF-Gly2752Ser in a dose-dependent manner

(Figure 5C, lysate). These results indicate that rVWF-Gly2752Ser has a weak dominant-negative effect to inhibit rVWF-WT multimer formation and extracellular secretion.

DISCUSSION

In the present study, we identified a novel genetic variation, *VWF* c.8254 G>A (p.Gly2752Ser), in a Japanese male patient diagnosed with type 3 VWD. Based on *ex vivo* ECFCs and *in vitro* rVWF expression system experiments, we revealed that VWF-Gly2752Ser caused dimerization impairment, resulting in its abnormal ER retention and defects in its extracellular secretion.

The phenotypic expression of VWF in heterozygotes in families is highly variable. The reason for this is that the relationship between VWD gene variants and phenotype is notoriously difficult to establish in type 1 and type 2 studies [38, 39], and certain variants may be diagnosed differently in different patients. This may be the reason for the phenotypic variability in the family studied here. In addition, as VWF is known to increase with age [40], parents with probands may be particularly affected. The large discrepancy between VWF:RCo and Ag in the two sons is even more difficult to understand. Ideally, the data should be confirmed by retesting, but unfortunately consent was not obtained.

Multimerization is normally a necessary process for VWF to serve its physiological function [1, 2]. VWF subunits are linked pairwise via interchain-disulfide bonds and subsequently form HMWMs [41]. In the ER, a newly synthesized VWF (preproVWF) is processed to a proVWF followed by forming an intermolecular C-terminal dimer with interchain-disulfide bonds of Cys2771-2773´, Cys2771´-2773, and Cys2811-2811´ in the CK domains [6] as suggested by chemical and mutational studies [4]. The proVWF C-terminal dimers are transported into the Golgi apparatus and further processed to form a multimeric molecule by N-terminal interchain disulfide bonds [7]. In C-terminal dimer formation, other non-disulfide bonds are also formed: interchain-hydrogen bonds (Cys2750-Ala2758 and Lys2810-Ser2812) and hydrophobic bonds (Tyr2749-Met2759 and Tyr2760-Ile2762-Val2767) [5]. Gly2752 is located between Cys2750 and

Cys2754 on the β4 strand in the CK domain and forms an interchain-hydrogen bond with Ser2756 of a counterpart VWF subunit (Figure 6) [5]. rVWF-Ser2756Ala, an alanine substitution variant at Ser2756 that disrupts the interchain-hydrogen bond between Gly2752 and Ser2756, shows an abnormal multimer pattern with higher-order multimers with extraneous intermediate bands, similar to the rVWF-Gly2752Ser variant. In addition, the rVWF-Ser2756Ala variant appears to have a far less significant effect on the VWF expression level, given its intensity on a multimer gel (Supplementary Figure 2). We consider that the Gly2752Ser substitution affects the C-terminal intermolecular interaction of VWF subunits, resulting in C-terminal dimer formation impairment.

However, the detection of trace amounts of VWF molecules in the patient's plasma (Figure 1 and Table 1) and cell culture media of rVWF-Gly2752Ser transfectants (Figure 3) indicate that there is VWF-Gly2752Ser with the size of two VWF units (dimer). One possibility is that VWF dimerization at the C-termini is not completely prevented. Tjernberg et al. reported that the type 3 VWD variant Cys2754Trp is mostly retained in the ER because of impairment of C-terminal dimer formation, though low amounts of VWF-Cys2754Trp are passed to the Golgi apparatus and subjected to multimer formation via N-terminal interchain disulfide bonds [19]. We therefore consider that VWF-Gly2752Ser can be dimerized via C-terminal interchain disulfide bonds at a very low rate within the ER and further be joined in the Golgi apparatus (Figure 7A). In this process, most of the dimerized VWF-Gly2752Ser must be subjected to further multimerization.

Plasma VWF multimers are modified by proteolytic cleavage with ADAMTS13, which generates N-terminal and C-terminal fragments [7, 8, 42, 43]. These cleaved fragments are known as the faster migrating satellite, intermediate triplet, and slower migrating satellite based on their mobility in multimer analysis using SDS-agarose gel electrophoresis [44, 45]. Fischer et al. proposed that the slower migrating satellite bands are composed of variable numbers of dimers

having one N-terminal fragment attached (Figure 7B-i) degraded from the tetramer, the intermediate triplet bands represent symmetric and/or asymmetric VWF dimers (Figure 7B-ii), and the faster migrating satellite bands are composed of variable numbers of dimers with one subunit lacking one N-terminal fragment (Figure 7B-iii) [45]. Our multimer analysis of VWF-Gly2752Ser in plasma showed an interesting and distinctive pattern that included only low molecular weight VWF representing the slower and faster satellites (Figure 1C). As an explanation of this distinct Gly2752Ser pattern, we consider that a tiny amount of tetramerized (and/or further multimerized) VWF-G2752S is proteolytically cleaved by ADAMTS13 in circulation and generates several forms of fragments: a dimer with one N-terminal fragment (slower migrating satellite, Figure 7B-iv) and a dimer with one subunit lacking the N-terminal fragment (faster migrating satellite, Figure 7B-vi). Disappearance of the intermediate triplet band for VWF-Gly2752Ser indicates that symmetric and/or asymmetric VWF dimers are consumed into faster migrating satellites and thus appear nonexistent or below the limit of detection (Figure 7B-v).

There are several limitations in this study. First, the lack of *ex vivo* investigation using patient-derived ECFCs. We captured bright-field and ICC images of patient-derived ECFCs (Figure 2). However, we were not able to further obtain ECFCs in sufficient amounts to investigate VWF synthesis, intracellular transport, and the secretion level. We previously succeeded in establishing patient-derived ECFCs and cryopreserved some of them. However, these cryopreserved cells did not completely recover, with their morphology and proliferation rate being significantly altered. The cytological properties of ECFC often depend on the characteristics of the donor [46]. Researchers should carefully handle cultures or cryopreserved ECFC cells in relation to their various cytological properties. Furthermore, the VE-cadherin signal was weakened in the patient-derived ECFCs. De Boer et al. reported that the VE-cadherin expression level was weakened in ECFC colonies with lower cell density that are observed [46]. De Jong et al.

described that expression of mesenchymal markers such as ACTA1, VIM, and COL1A1 were increased in ECFCs with low cell density suggesting that Endo-MT (endothelial-mesenchymal transition) is the cause of the variation in ECFCs [47]. In this study, in spite of repeated tries to newly generate patient-derived ECFCs, ECFC colonies with higher cell density were not obtained. Second, expression studies that in VWF-transfected COS-7 [16, 48-49] and HEK293 [50] cells, higher-order multimers are detected in the culture medium but not in cell lysates. Lyons et al. described that the intracellular processing speed of VWF molecule could explain this phenomenon. After dimerized VWFs exit from the ER, VWF molecules are rapidly multimerized and transported through the Golgi apparatus to be secreted [16]. These reports shown that VWF from cell lysates predominantly consists of low-molecular weight VWF molecules, rather than the full range of multimers seen in cell culture medium or plasma. These reports are consistent with the observations shown in Figure 3B (lysate) and 5B (lysate). However, rVWF-WT showed a multimeric structure in the transfectant culture medium (Figure 3B and 5B). This observation reveals that our VWF expression system can mimic the intracellular VWF processing.

In conclusion, we investigated a novel VWF variant, VWF-Gly2752Ser, and demonstrated its molecular pathogenesis, which is secretory impairment due to the hampering of C-terminal dimer formation. VWF-Gly2752Ser causes the severe reduction of circulating VWF:Ag levels, but not a null phenotype. The very low amount of circulating VWF-Gly2752Ser is likely to be a tetramer (and/or further multimerized), which accounts for the patient's clinical phenotypes: slightly higher FVIII levels (FVIII: C 11%) and mild or moderate bleeding episodes. As shown in Figure 3B, rVWF-Gly2752Ser was secreted in very low amounts. Based on a report by the subcommittee on VWF in ISTH [51, 52], the phenotype of VWF-Gly2752Ser is categorized as type 3 VWD, which is caused by clinically recessive variations usually associated with undetectable VWF levels (< 5 IU/dL), although VWF-Gly2752Ser appeared to have a weak

dominant-negative effect (Figure 5). To the best of our knowledge, the present study is the first report of type 3 VWD caused by a missense variation associated with a non-cysteine substitution. Additional screening investigations of genetic variations, especially missense variations in the CK domain, will contribute to further understanding of the pathological molecular basis of type 3 VWD.

ACKNOWLEDGMENTS

We thank Drs. Masaki Hayakawa and Masanori Matsumoto (Department of Blood Transfusion Medicine, Nara Medical University, Kashihara, Japan) for instruction of multimer analysis, and Mrs. Chika Wakamatsu for her excellent molecular biological work.

AUTHORSHIP CONTRIBUTIONS

S. Okamoto, S. Tamura and N. Suzuki designed and performed the research, analyzed the data, and drafted the manuscript. N. Sanda, K. Odaira, Y. Hayakawa, M. Mukaide, A. Suzuki and T. Kanematsu conducted the research and analyzed the data. A. Katsumi, F. Hayakawa, H. Kiyoi and T. Kojima developed the project. T. Matsushita designed the project, analyzed the data, and drafted the manuscript.

CONFLICTS OF INTEREST

The authors declare no conflicts of interest exist that are associated with this manuscript.

FIGURE LEGENDS

Figure 1. Genotype and molecular phenotype of VWF-Gly2752Ser

A) Family tree of the patient. The patient (II-2) is indicated by an arrow. B) Direct sequencing analysis identified a guanine-to-adenine substitution at nucleotide 8254 (c.8254 G>A). The variation was detected as a single peak in the patient's genomic DNA (arrow). C) VWF multimer analysis by SDS-agarose gel electrophoresis. NP: normal plasma, Pt: patient plasma. Closed and opened arrowheads indicate faster- and slower-migrating satellites of VWF molecules, respectively. The numbers at the left side of the image indicate the subunit number of each VWF multimer molecule. D) Non-reducing SDS-PAGE/WB of plasma VWF. NP: normal plasma, Pt: patient plasma. The band near 500 kDa indicates dimerized VWF.

Figure 2. *Ex vivo* VWF production analysis by patient-derived endothelial colony forming cells (ECFCs)

A) Representative microscopic image of ECFCs at low (4-fold) and high (10-fold) magnification of the objective lens. Scale bar, 100 μm at low and 40 μm at high magnification. B) Representative confocal microscopic images of ECFCs stained for VWF (green) and VE-cadherin (red). In the image of ECFCs derived from the patient. HC: healthy control, Pt: patient. Scale bar, 12.5 μm for HC and 25 μm for Pt.

Figure 3. *In vitro* analysis of VWF-Gly2752Ser by the recombinant VWF (rVWF) expression system

A) Quantitative rVWF levels in the culture medium and lysate of transfectants with rVWF-WT or Gly2752Ser expression vectors. The rVWF level is normalized to rVWF-WT as 100%. The error

bars indicate SEM values calculated from five independent experiments. **P < 0.01 and *** P < 0.001 vs. WT as determined by Student's *t* test. B) Multimer analysis of rVWF by SDS-agarose electrophoresis in the culture medium and lysate of transfectants with rVWF-WT or Gly2752Ser expression vectors. The numbers at the left of the image indicate the subunit number of each rVWF multimer molecule. In the image of the cell culture medium, opened and closed arrowheads indicate the bands representing dimeric and tetrameric rVWF, respectively. C) Non-reducing SDS-PAGE/WB of rVWF in the culture medium and lysate of transfectants with rVWF-WT or G2752S expression vectors. The bands near 250 kDa and 500 kDa indicate monomeric and dimeric rVWF, respectively.

Figure 4. Subcellular localization analysis of rVWF-Gly2752Ser by fluorescence microscopy

A) Colocalization analysis of rVWF-Gly2752Ser (green) and the ER (PDI**,** red). B) PCC analysis of rVWF and ER. C) Colocalization analysis of rVWF-Gly2752Ser (red) and the Golgi apparatus (green). D) PCC analysis of rVWF and the Golgi apparatus. Cell nuclei were stained with DAPI (blue). Scale bar, 10 μm. The PCC score was calculated using at least ten cells for each rVWF transfectant. The error bars indicate SD values. *** P < 0.001 vs. WT as determined by Student's *t* test.

Figure 5. Co-transfection analysis of rVWF-WT and Gly2752Ser

A) Experimental design showing mixing ratios of rVWF-WT and Gly2752Ser expression vectors. B) Multimer analysis of co-transfected rVWF in the cell culture medium and lysate. The numbers at the left of the image indicate the subunit number of each rVWF multimer. C) Quantitative analysis of co-transfected rVWF in the cell culture medium and lysate. The graphs are normalized

to the vector mixing condition (i) shown as panel A. The error bars indicate SEM values calculated from five independent experiments.

* $P < 0.001$ vs. the mixing condition (i) detected by one-way ANOVA in the cell culture medium.

$^{\#}P < 0.05$, $^{\#\#}P < 0.001$ vs. the mixing condition (i) detected by one-way ANOVA in the cell lysate.

Figure 6. Alignment of the Gly2752 flanking region in the CK domain β4 strand.

Gly2752 (shown in red) is located between Cys2750 and Cys2754 on the β4 strand in the CK domain. Gly2752 forms an interchain hydrogen bond (shown as blue solid lines) with Ser2756 of a counterpart VWF subunit (β4′). Tyr2749 forms an intrachain hydrophobic bond with Met2759 (brown dotted line). Cysteine residues (Cys2750 and Cys2754) that contribute to intrachain disulfide bonds are shown as green squares.

Figure 7. Putative pathogenic mechanism of VWF-Gly2752Ser

A) Putative intracellular structure and transport behavior of VWF-G2752S. Newly synthesized VWF-Gly2752Ser subunits are dimerized via C-terminal interchain disulfide bonds at a very low rate within the ER, and further joined via N-terminal interchain disulfide bonds in the Golgi apparatus. In this process, most dimerized VWF-Gly2752Ser must be subjected to tetramerization (and/or further multimerization). B) Putative triplet and satellite structures of plasma VWF-WT or Gly2752Ser according to multimer analysis using SDS-agarose electrophoresis. The slower migrating satellite bands are composed of variable numbers of dimers having one N-terminal fragment attached (i and iv). The intermediate triplet bands represent symmetric and/or asymmetric VWF dimers (ii and v). The faster migrating satellite bands are composed of variable numbers of dimers with one subunit lacking one N-terminal fragment (iii and vi). Plasma

VWF-Gly2752Ser shows an interesting and distinctive pattern with only the slower and faster satellite bands.

Supplementary Figure 1. Multimer analysis of rVWF-Cys1099Ala/Cys1142Ala and rVWF-Cys1099Ala/Cys1142Ala/Gly2752Ser variants.

In the rVWF-Cys1099Ala/Cys1142Ala variant, a dimer form interlinked via only C-terminal disulfide bonds was detected. In rVWF-Cys1099Ala/Cys1142Ala/Gly2752Ser, a dimer and monomer, which is consistent with the multimer pattern of rVWF-Gly2752Ser, were detected. The numbers at the left of the image indicate the subunit number of each rVWF multimer.

Supplementary Figure 2. Multimer analysis of rVWF-Ser2756Ala and rVWF-Gly2752Ser/Ser2756Ala variants.

rVWF-Ser2756Ala showed an abnormal multimer pattern that is higher order multimers with extraneous intermediate bands like the rVWF-Gly2752Ser variant.

rVWF-Gly2752Ser/Ser2756Ala also showed an abnormal multimer pattern like the rVWF-Gly2752Ser variant. These results suggest that the disruption of interchain hydrogen bonds between Gly2752 and Ser2756 causes C-terminal dimer formation impairment.

References

1 Sadler JE. Biochemistry and genetics of von Willebrand factor. *Annu Rev Biochem*. 1998;**67**:395-424. 10.1146/annurev.biochem.67.1.395.

2 Lenting PJ, Christophe OD, Denis CV. von Willebrand factor biosynthesis, secretion, and clearance: connecting the far ends. *Blood*. 2015;**125**:2019-2028. 10.1182/blood-2014-06-528406.

3 Marti T, Rösselet SJ, Titani K, Walsh KA. Identification of disulfide-bridged substructures within human von Willebrand factor. *Biochemistry*. 1987;**26**:8099-8109. 10.1021/bi00399a013.

4 Katsumi A, Tuley EA, Bodó I, Sadler JE. Localization of disulfide bonds in the cystine knot domain of human von Willebrand factor. *J Biol Chem*. 2000;**275**:25585-25594. 10.1074/jbc.M002654200.

5 Zhou YF, Springer TA. Highly reinforced structure of a C-terminal dimerization domain in von Willebrand factor. *Blood*. 2014;**123**:1785-1793. 10.1182/blood-2013-11-523639.

6 Lippok S, Kolšek K, Löf A, Eggert D, Vanderlinden W, Müller JP, König G, Obser T, Röhrs K, Schneppenheim S, Budde U, Baldauf C, Aponte-Santamaría C, Gräter F, Schneppenheim R, Rädler JO, Brehm MA. von Willebrand factor is dimerized by protein disulfide isomerase. *Blood*. 2016;**127**:1183-1191. 10.1182/blood-2015-04-641902.

7 Purvis AR, Gross J, Dang LT, Huang RH, Kapadia M, Townsend RR, Sadler JE. Two Cys residues essential for von Willebrand factor multimer assembly in the Golgi. *Proc Natl Acad Sci U S A*. 2007;**104**:15647-15652. 10.1073/pnas.0705175104.

8 Huang RH, Wang Y, Roth R, Yu X, Purvis AR, Heuser JE, Egelman EH, Sadler JE. Assembly of Weibel-Palade body-like tubules from N-terminal domains of von Willebrand factor. *Proc Natl Acad Sci U S A*. 2008;**105**:482-487. 10.1073/pnas.0710079105.

9 Zhou YF, Eng ET, Nishida N, Lu C, Walz T, Springer TA. A pH-regulated dimeric bouquet in the structure of von Willebrand factor. *EMBO J*. 2011;**30**:4098-4111.

10.1038/emboj.2011.297.

10 Furlan M, Robles R, Galbusera M, Remuzzi G, Kyrle PA, Brenner B, Krause M, Scharrer I, Aumann V, Mittler U, Solenthaler M, Lämmle B. von Willebrand factor-cleaving protease in thrombotic thrombocytopenic purpura and the hemolytic-uremic syndrome. *N Engl J Med*. 1998;**339**:1578-1584. 10.1056/NEJM199811263392202.

11 Tsai HM, Lian EC. Antibodies to von Willebrand factor-cleaving protease in acute thrombotic thrombocytopenic purpura. *N Engl J Med*. 1998;**339**:1585-1594. 10.1056/NEJM199811263392203.

12 Dent JA, Galbusera M, Ruggeri ZM. Heterogeneity of plasma von Willebrand factor multimers resulting from proteolysis of the constituent subunit. *J Clin Invest*. 1991;**88**:774-782. 10.1172/JCI115376.

13 Zheng X, Chung D, Takayama TK, Majerus EM, Sadler JE, Fujikawa K. Structure of von Willebrand factor-cleaving protease (ADAMTS13), a metalloprotease involved in thrombotic thrombocytopenic purpura. *J Biol Chem*. 2001;**276** 41059-41063. 10.1074/jbc.C100515200.

14 De Ceunynck K, De Meyer SF, Vanhoorelbeke K. Unwinding the von Willebrand factor strings puzzle. *Blood*. 2013;**121**:270-277. 10.1182/blood-2012-07-442285.

15 de Jong A, Eikenboom J. Von Willebrand disease mutation spectrum and associated mutation mechanisms. *Thromb Res*. 2017;**159**:65-75. 10.1016/j.thromres.2017.09.025.

16 Lyons SE, Bruck ME, Bowie EJ, Ginsburg D. Impaired intracellular transport produced by a subset of type IIA von Willebrand disease mutations. *J Biol Chem*. 1992;**267**:4424-4430.

17 Schneppenheim R, Budde U, Obser T, Brassard J, Mainusch K, Ruggeri ZM, Schneppenheim S, Schwaab R, Oldenburg J. Expression and characterization of von Willebrand factor dimerization defects in different types of von Willebrand disease. *Blood*. 2001;**97**:2059-2066. 10.1182/blood.v97.7.2059.

18 Tjernberg P, Vos HL, Castaman G, Bertina RM, Eikenboom JC. Dimerization and multimerization defects of von Willebrand factor due to mutated cysteine residues. *J Thromb Haemost*. 2004;**2**:257-265. 10.1111/j.1538-7836.2003.00435.x.

19 Tjernberg P, Vos HL, Spaargaren-van Riel CC, Luken BM, Voorberg J, Bertina RM, Eikenboom JC. Differential effects of the loss of intrachain- versus interchain-disulfide bonds in the cystine-knot domain of von Willebrand factor on the clinical phenotype of von Willebrand disease. *Thromb Haemost*. 2006;**96**:717-724. 10.1160/th06-08-0460.

20 Wang JW, Valentijn KM, de Boer HC, Dirven RJ, van Zonneveld AJ, Koster AJ, Voorberg J, Reitsma PH, Eikenboom J. Intracellular storage and regulated secretion of von Willebrand factor in quantitative von Willebrand disease. *J Biol Chem*. 2011;**286**:24180-24188. 10.1074/jbc.M110.215194.

21 Kitchen S, McCraw AH, Echenagucia M. *Diagnosis of Hemophilia and Other Bleeding Disorders. A LABORATORY MANUAL Second Edition*. 2010

22 Ormiston ML, Toshner MR, Kiskin FN, Huang CJ, Groves E, Morrell NW, Rana AA. Generation and Culture of Blood Outgrowth Endothelial Cells from Human Peripheral Blood. *J Vis Exp*. 2015;**106**:e53384. 10.3791/53384.

23 Hayakawa Y, Tamura S, Suzuki N, Odaira K, Tokoro M, Kawashima F, Hayakawa F, Takagi A, Katsumi A, Suzuki A, Okamoto S, Kanematsu T, Matsushita T, Kojima T. Essential role of a carboxyl-terminal alpha-helix motif in the secretion of coagulation factor XI. *J Thromb Haemost*. 2021;**19**:920-930. 10.1111/jth.15242.

24 Matsushita T, Sadler JE. Identification of amino acid residues essential for von Willebrand factor binding to platelet glycoprotein Ib. Charged-to-alanine scanning mutagenesis of the A1 domain of human von Willebrand factor. *J Biol Chem*. 1995;**270**:13406-13414. 10.1074/jbc.270.22.13406.

25 Burke RL, Pachl C, Quiroga M, Rosenberg S, Haigwood N, Nordfang O, Ezban M. The functional domains of coagulation factor VIII:C. *J Biol Chem*. 1986;**261**:12574-12578.

26 Rodeghiero F, Tosetto A, Abshire T, Arnold DM, Coller B, James P, Neunert C, Lillicrap D; ISTH/SSC joint VWF and Perinatal/Pediatric Hemostasis Subcommittees Working Group. ISTH/SSC bleeding assessment tool: a standardized questionnaire and a proposal for a new bleeding score for inherited bleeding disorders. *J Thromb Haemost.* 2010; **8**: 2063-2065. 10.1111/j.1538-7836.2010.03975.x.

27 Kircher M, Witten DM, Jain P, O'Roak BJ, Cooper GM, Shendure J. A general framework for estimating the relative pathogenicity of human genetic variants. *J.Nat Genet.* 2014; **46**: 310-315. 10.1038/ng.2892.

28 Rentzsch P, Witten D, Cooper GM, Shendure J, Kircher M. CADD: predicting the deleteriousness of variants throughout the human genome. *Nucleic Acids Res*. 2019;**47** D886-D894. 10.1093/nar/gky1016.

29 Grantham R. Amino acid difference formula to help explain protein evolution *Science*. 1974;**185**:862-864. 10.1126/science.185.4154.862.

30 Borchiellini A, Fijnvandraat K, ten Cate JW, Pajkrt D, van Deventer SJ, Pasterkamp G, Meijer-Huizinga F, Zwart-Huinink L, Voorberg J, van Mourik JA. Quantitative analysis of von Willebrand factor propeptide release in vivo: effect of experimental endotoxemia and administration of 1-deamino-8-D-arginine vasopressin in humans. *Blood*. 1996;**88**:2951-2958.

31 Ng C, Motto DG, Di Paola J. Diagnostic approach to von Willebrand disease. *Blood*. 2015;**125**:2029-2037. 10.1182/blood-2014-08-528398.

32 Matsui T, Titani K, Mizuochi T.Structures of the asparagine-linked oligosaccharide chains of human von Willebrand factor. Occurrence of blood group A, B, and H(O) structure. *J Biol Chem*.1992;**267**:8723-8731.

33 Ingram DA, Mead LE, Tanaka H, Meade V, Fenoglio A, Mortell K, Pollok K, Ferkowicz MJ, Gilley D, Yoder MC. Identification of a novel hierarchy of endothelial progenitor cells using human peripheral and umbilical cord blood. *Blood*. 2004;**104**:2752-2760. 10.1182/blood-2004-04-1396.

34 Smadja DM, Melero-Martin JM, Eikenboom J, Bowman M, Sabatier F, Randi AM. Standardization of methods to quantify and culture endothelial colony-forming cells derived from peripheral blood: Position paper from the International Society on Thrombosis and Haemostasis SSC. *J Thromb Haemost*. 2019;**17:**1190-1194. 10.1111/jth.14462.

35 Brehm MA, Huck V, Aponte-Santamaría C, Obser T, Grässle S, Oyen F, Budde U, Schneppenheim S, Baldauf C, Gräter F, Schneider SW, Schneppenheim R. von Willebrand disease type 2A phenotypes IIC, IID and IIE: A day in the life of shear-stressed mutant von Willebrand factor. *Thromb Haemost.* 2014;**112**:96-108. 10.1160/TH13-11-0902.

36 Obser T, Ledford-Kraemer M, Oyen F, Brehm MA, Denis CV, Marschalek R, Montgomery RR, Sadler JE, Schneppenheim S, Budde U, Schneppenheim R. Identification and characterization of the elusive mutation causing the historical von Willebrand Disease type IIC Miami. *J Thromb Haemost*. 2016;**14**:1725-1735. 10.1111/jth.13398.

37 Yadegari H, Biswas A, Ahmed S, Naz A, Oldenburg J. von Willebrand factor propeptide missense variants affect anterograde transport to Golgi resulting in ER retention. *Hum Mutat*. 2021;**42**:731-744. 10.1002/humu.24204.

38 Robertson JD, Yenson PR, Rand ML, Blanchette VS, Carcao MD, Notley C, Lillicrap D, James PD. Expanded phenotype-genotype correlations in a pediatric population with type 1 von Willebrand disease. *J Thromb Haemost*. 2011;**9**:1752-1760. 10.1111/j.1538-7836.2011.04423.x.

39 DiGiandomenico S, Christopherson PA, Haberichter SL, Abshire TC, Montgomery RR, Flood VH; Zimmerman Program Investigators. Laboratory variability in the diagnosis of type 2 VWD variants. *J Thromb Haemost*. 2021;**19**:131-138. 10.1111/jth.15129.

40 Seaman CD, Ragni MV. The Association of Aging With Von Willebrand Factor Levels and Bleeding Risk in Type 1 Von Willebrand Disease. *Clin Appl Thromb Hemost.* 2018;**24**:434-438. 10.1177/1076029617724232.

41 Springer TA. Biology and physics of von Willebrand factor concatamers. *J Thromb Haemost.* 2011;**9**:130-143. 10.1111/j.1538-7836.2011.04320.x.

42 Ledford-Kraemer MR. Analysis of von Willebrand factor structure by multimer analysis. *Am J Hematol*. 2010;**85**:510-514. 10.1002/ajh.21739.

43 Kannicht C, Fisseau C, Hofmann W, Kröning M, Fuchs B. ADAMTS13 content and VWF multimer and triplet structure in commercially available VWF/FVIII concentrates. *Biologicals*. 2015;**43**:117-122. doi: 10.1016/j.biologicals.2014.11.006

44 Furlan M, Robles R, Affolter D, Meyer D, Baillod P, Lämmle B. Triplet structure of von Willebrand factor reflects proteolytic degradation of high molecular weight multimers. *Proc Natl Acad Sci U S A*. 1993;**90**:7503-7507. 10.1073/pnas.90.16.7503.

45 Fischer BE, Thomas KB, Schlokat U, Dorner F. Triplet structure of human von Willebrand factor. *Biochem J*. 1998;**331**:483-488. 10.1042/bj3310483.

46 de Boer S, Bowman M, Notley C, Mo A, Lima P, de Jong A, Dirven R, Weijers E, Lillicrap D, James P, Eikenboom J. Endothelial characteristics in healthy endothelial colony forming cells; generating a robust and valid ex vivo model for vascular disease. *J Thromb Haemost*. 2020;**18:**2721-2731. 10.1111/jth.14998.

47 de Jong A, Weijers E, Dirven R, de Boer S, Streur J, Eikenboom J. Variability of von Willebrand factor-related parameters in endothelial colony forming cells. *J Thromb Haemost.* 2019;**17:**1544-1554. 10.1111/jth.14558.

48 Mayadas TN, Wagner DD. Vicinal cysteines in the prosequence play a role in von Willebrand factor multimer assembly. *Proc Natl Acad Sci U S A*. 1992;**89**:3531-3535. 10.1073/pnas.89.8.3531.

49 Baronciani L, Federici AB, Cozzi G, La Marca S, Punzo M, Rubini V, Canciani MT, Mannucci PM. Expression studies of missense mutations p.D141Y, p.C275S located in the propeptide of von Willebrand factor in patients with type 3 von Willebrand disease. *Haemophilia* .2008;**14**:549-555. 10.1111/j.1365-2516.2008.01682.x.

50 Michaux G, Hewlett LJ, Messenger SL, Goodeve AC, Peake IR, Daly ME, Cutler DF. Analysis of intracellular storage and regulated secretion of 3 von Willebrand disease-causing variants of von Willebrand factor. *Blood*. 2003;**102**:2452-2458. 10.1182/blood-2003-02-0599.

51 Nichols WL, Hultin MB, James AH, Manco-Johnson MJ, Montgomery RR, Ortel TL, Rick ME, Sadler JE, Weinstein M, Yawn BP. von Willebrand disease (VWD): evidence-based diagnosis and management guidelines, the National Heart, Lung, and Blood Institute (NHLBI) Expert Panel report (USA). *Haemophilia*. 2008;**14**:171-232. 10.1111/j.1365-2516.2007.01643.x

52 James PD, Connell NT, Ameer B, Di Paola J, Eikenboom J, Giraud N, Haberichter S, Jacobs-Pratt V, Konkle B, McLintock C, McRae S, R Montgomery R, O'Donnell JS, Scappe N, Sidonio R, Flood VH, Husainat N, Kalot MA, Mustafa RA. ASH ISTH NHF WFH 2021 guidelines on the diagnosis of von Willebrand disease. *Blood Adv*. 2021;**5**:280-300. 10.1182/bloodadvances.2020003265.

Table 1. Hematological data of the patient and his family.

	I–1 (Father)	I–2 (Mother)	II–2 (Patient)	III-1 (Eldest son)	III-2 (Second son)
Age (years)	88	85	49	13	11
Blood type	B	AB	AB	B	AB
VWF:Ag (%)	120	111	< 5	82	40
VWF:Ag (μg/mL)	–	–	0.12	–	–
VWF:RCo (%)	142	130	< 6	79	42
FVIII:C (%)	> 150	137.5	11	135.8	66.2
ISTH-BATs score	0	0	8	0	0

VWF:Ag, vonWillebrand factor antigen

VWF:RCo, von Willebrand factor ristocetin cofactor activity

FVIII, Factor VIII concentration

Figure 1

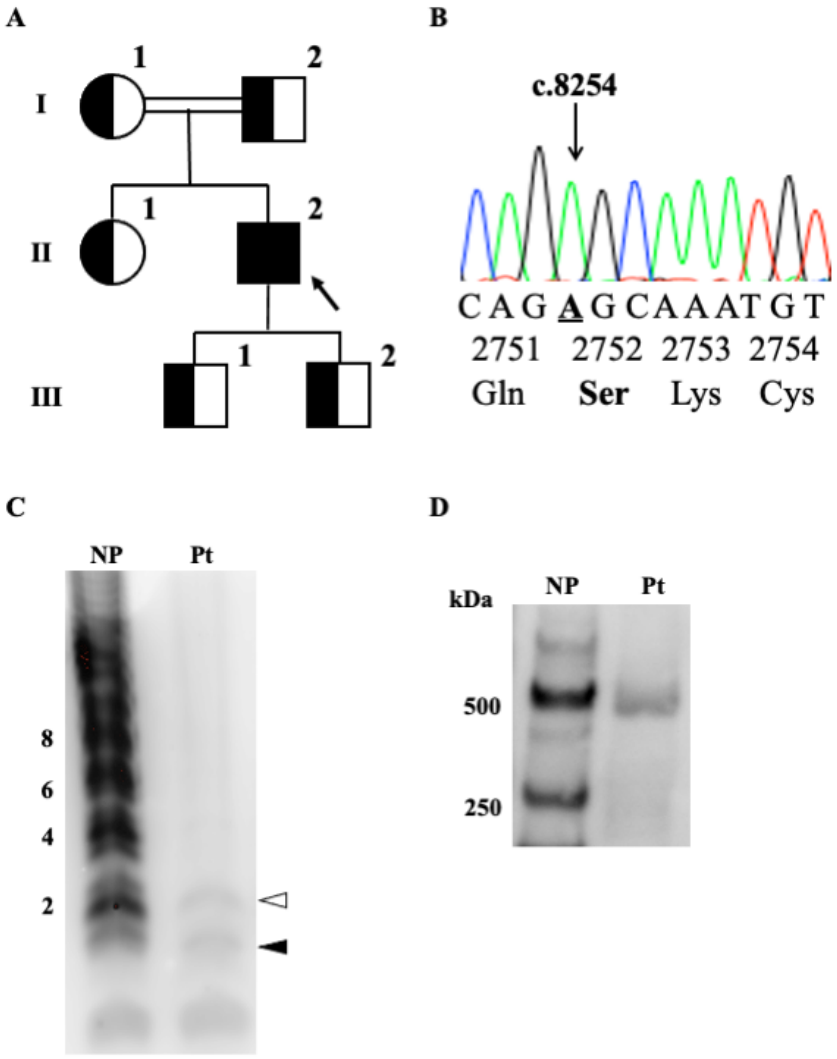

jth_15746_f1.tiff

Figure 2

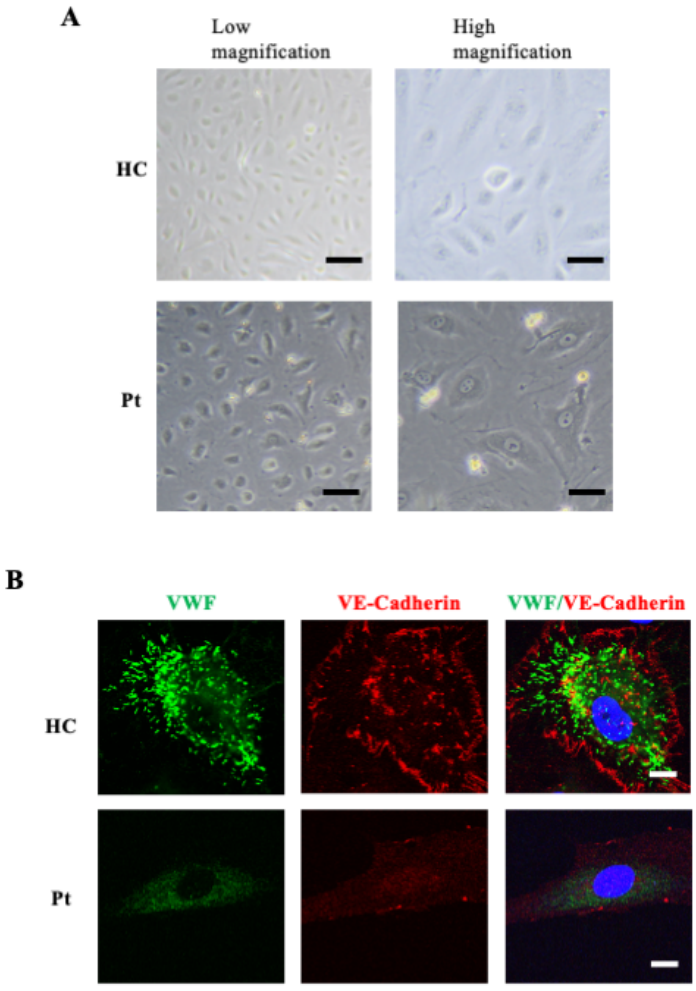

jth_15746_f2.tiff

Figure 3

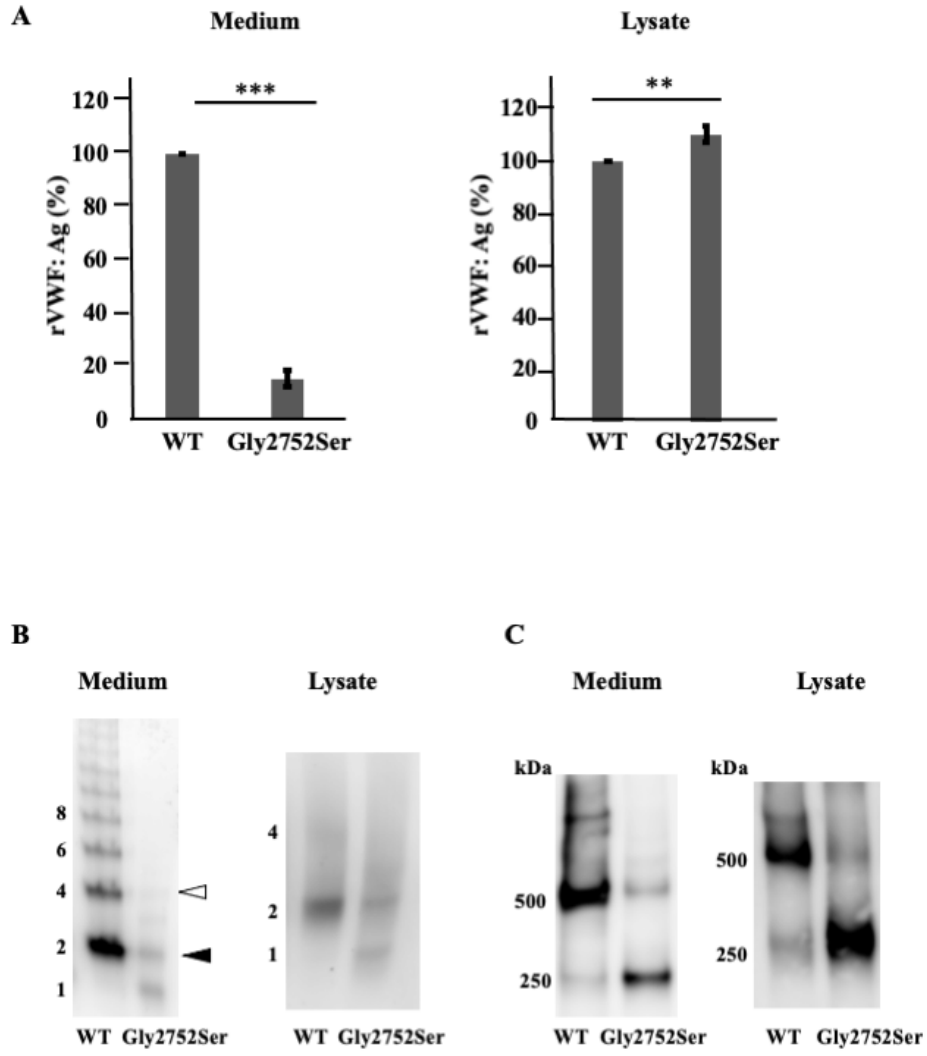

jth_15746_f3.tiff

Figure 4

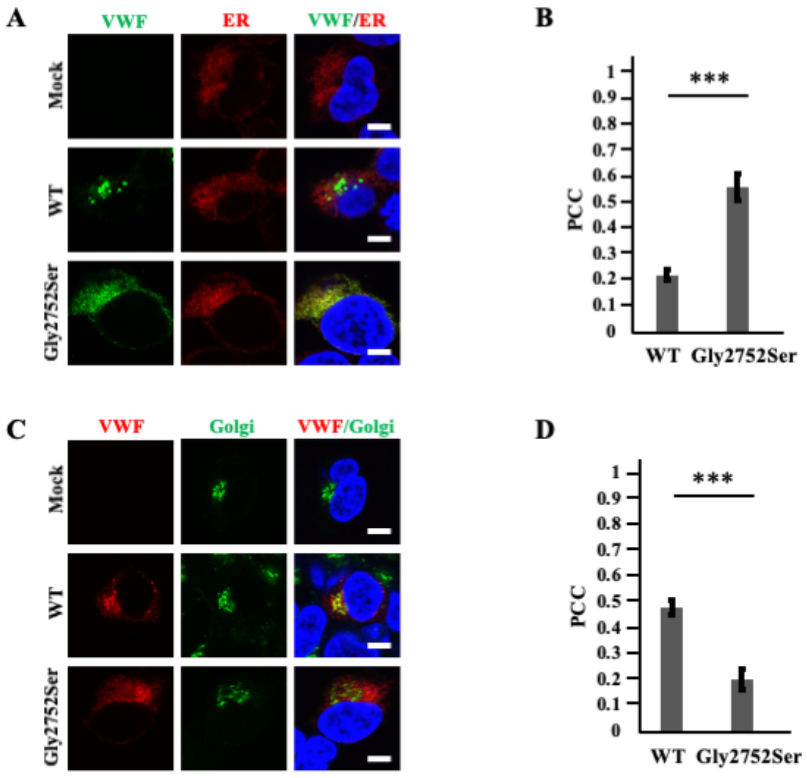

jth_15746_f4.tiff

Figure 5

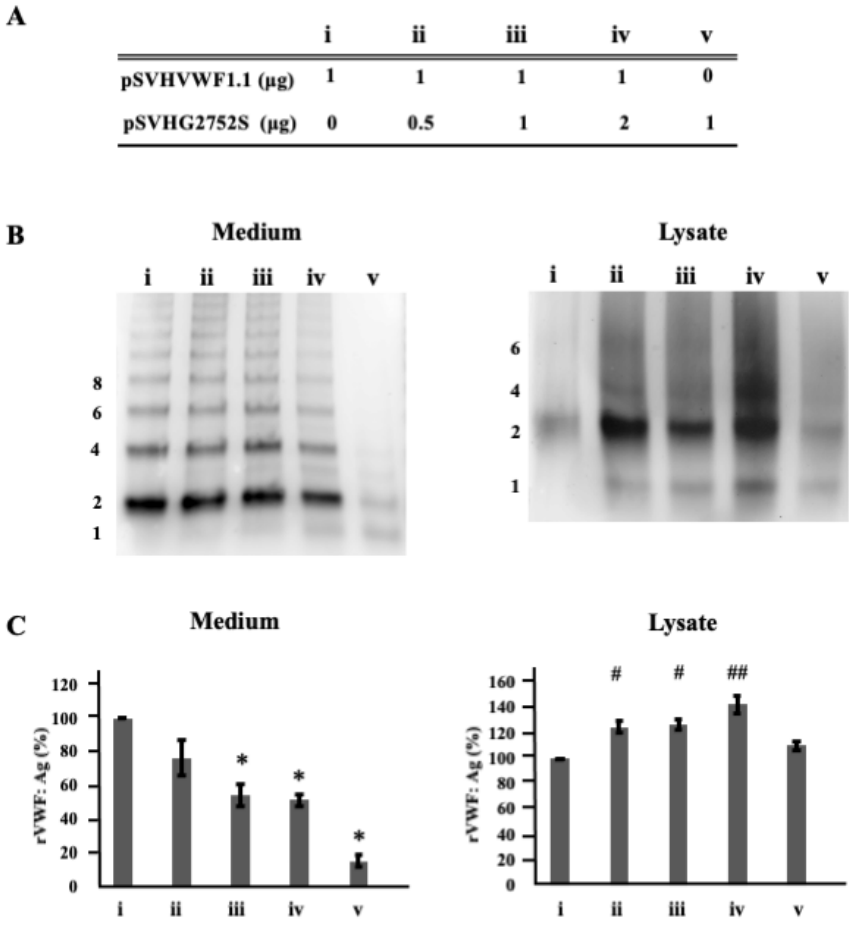

jth_15746_f5.tiff

Figure 6

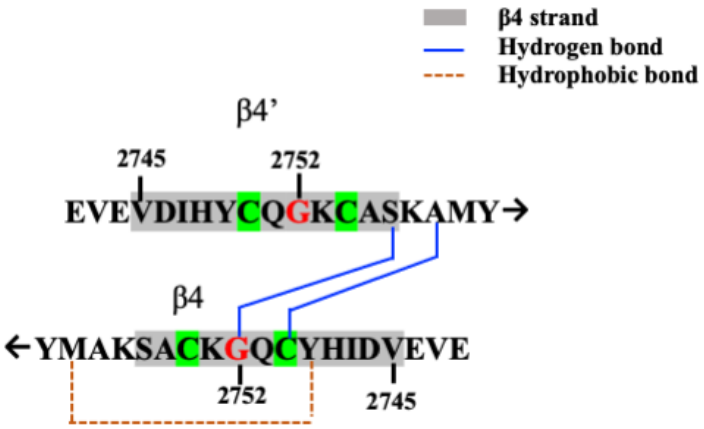

jth_15746_f6.tiff

Figure 7

A

	VWF monomer	Dimerization		Multimer structure
		C-terminal in ER	N-terminal in Golgi	
WT		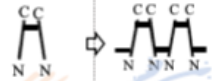		
p.Gly2752Ser				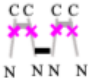

B

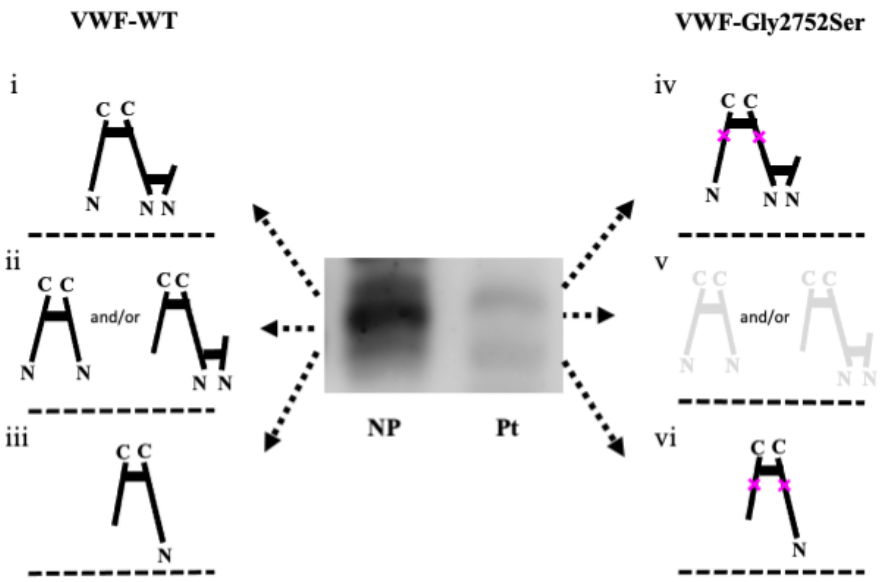

jth_15746_f7.tiff

Supplementary information

VWF ELISA

We used polyclonal rabbit anti-human VWF antibody (ab6994, Abcam, Cambridge, UK) as the primary antibody and anti-human VWF horseradish peroxidase-conjugated rabbit anti-human VWF antibody (P0226, DAKO, Carpinteria, California, USA) as the secondary antibody. Primary antibody diluted to 1:2000 with 0.05 M carbonate buffer (pH 9.6) was added to each well and incubated at 4 °C overnight. Standard plasma and samples were diluted with 0.3% bovine serum albumin (BSA; Sigma-Aldrich, St. Louis, Missouri, USA)-phosphate buffered saline (PBS). One hundred microliters of each diluted analyte were added to each well followed by incubation for 2 h at room temperature. Secondary antibody diluted to 1:2000 with 0.3% BSA-PBS was added to each well and incubated for 1 h. For the substrate solution, 2 mg of 1,2-orthophenylenediamine dichloride (OPD Tablet, FUJI FILM Wako Pure Chemical, Osaka, Japan) was dissolved in 0.1 M citrate phosphate buffer (pH 5.0), and 0.6 μL of hydrogen peroxide (MITSUBISHI GAS CHEMICAL COMPANY, Tokyo, Japan) was added. To stop color development, 1 M sulfuric acid (Sigma-Aldrich) was added, and the optical density at 492 nm was measured by microplate reader MPR4Ai (Tosoh, Tokyo, Japan).

VWF multimer analysis

A sample was diluted to an appropriate concentration with multimer analyzing sample buffer (10 mM Tris, 1 mM EDTA, 0.2% SDS, 0.8 M urea, pH 8.0) and subjected to 1.8% SDS-agarose gel electrophoresis. Electrophoresis was performed using electrode buffer (20 mM Tris, 20 mM glycine, 0.1% SDS, pH 8.35) and a Hoefer HE99X-15-1.5 (Hoefer, Holliston, Massachusetts, USA) with 20 mA constant current for 1 h, then 4 mA for 20 h at 4 °C. After electrophoresis, the gel was washed and dried. After blocking by 1% skim milk for 90 min, the gel was placed into primary antibody solution overnight followed by washing with Tris buffered saline (TBS)-0.05% Tween. The washed gel was placed into secondary antibody solution for 12 h.

VWF SDS-PAGE/WB

Samples were denatured with SDS-PAGE sample buffer (10 mM Tris, 2% SDS, 1.2 M urea, 15% glycerol, pH 6.8) and heating at 65 °C for 15 min. Denatured samples were electrophoresed under non-reducing conditions using NuPAGE® 3%–8%, Tris-Acetate Gel (Thermo Fisher Scientific, Waltham, Massachusetts, USA), NuPAGE™ Tris-Acetate SDS Running Buffer, and XCell SureLock™ (Thermo Fisher Scientific) according to the manufacturer's instructions, and transferred onto an Immune blot® PVDF membrane (Bio-Rad,

Hercules, California, USA) by a Trans-Blot® SD Semi-Dry Transfer Cell (Bio-Rad). Transferred membranes were incubated in 1% skim milk for 3 h. In both multimer analysis and SDS-PAGE, for VWF detection, we used horseradish peroxidase-conjugated rabbit anti-human VWF antibody (P0226, DAKO) and Amersham™ ECL prime Western Blotting Detection Reagent (GE Healthcare, Illinois, Chicago, USA). The VWF signal was captured by an LAS4000 (Fujifilm Tokyo Japan). As a loading control for SDS-PAGE, α/β-tubulin was detected with anti-α/β-Tubulin antibody #2148 (Cell Signaling Technology Danvers, Massachusetts, USA) and Anti-Rabbit IgG, HRP-Linked F(ab')2 Fragment Donkey (NA9340, GE Healthcare). Samples of cultured medium and cell lysate were collected by the procedures described in the Materials and Methods.

Supplementary Figure 1

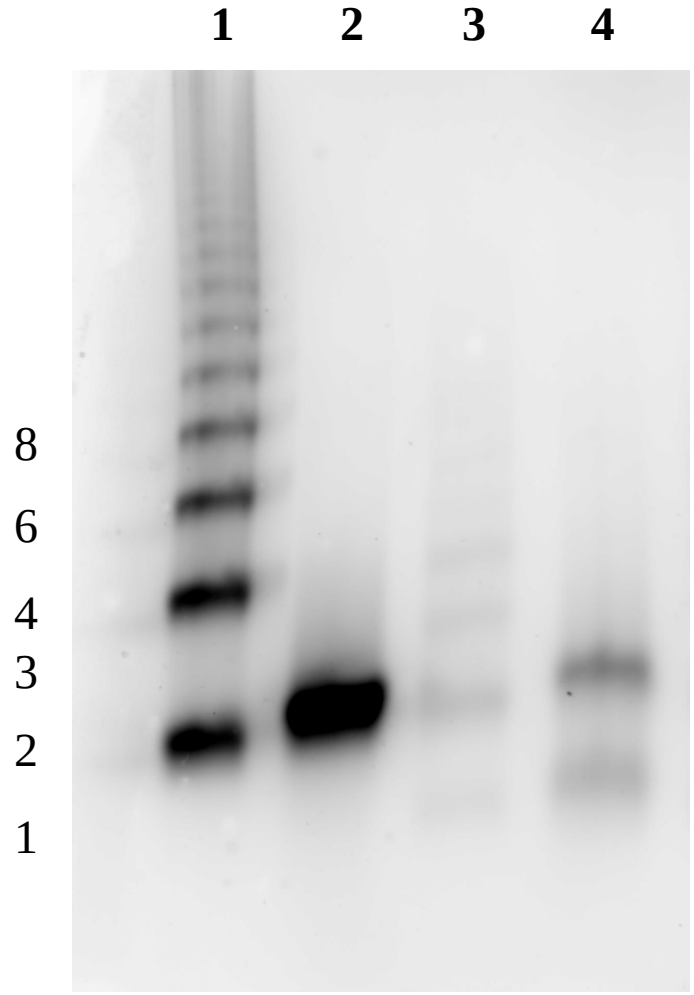

Lane 1: rVWF-WT
Lane 2: rVWF-Cys1099Ala/Cys1142Ala
Lane 3: rVWF-Gly2752Ser
Lane 4: rVWF-Cys1099Ala/Cys1142Ala/Gly2752Ser

Supplementary Figure 2

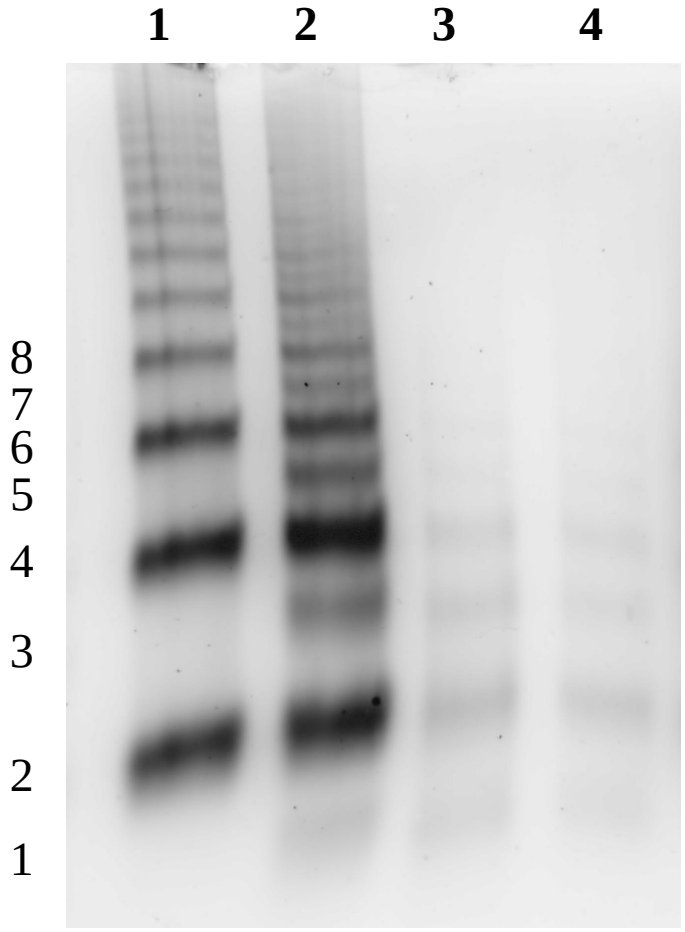

Lane 1: rVWF-WT
Lane 2: rVWF-Ser2756Ala
Lane 3: rVWF-Gly2752Ser
Lane 4: rVWF-Gly2752Ser/Ser2756Ala

Supplementary Table 1. Primers for experiments

Name of primer	Length	Sequence	Position	Application
VWF 52 U	19	5'-GAGGGGGTCAGGGAGAAAG-3'	5,949,281–5,949,299	PCR and sequencing *
VWF 52 L	20	5'-AACCGGTCTCAGAACTCAGC-3'	5,948,807–5,948,826	PCR and sequencing *
VWF_G2752S_Fw	28	5'-TGTGCCAGCAAAGCCATGTACTCCATTG-3'	8,260–8,287	Mutagenesis #
VWF_G2752S_Rv	30	5'-TTTGC**T**CTGGCAGTAGTGGATATCCACCTC-3'	8,230–8,259	Mutagenesis #
VWF_C1099A_Fw	30	5'-GCTGCCTATGCCCACGTGTGTGCCCAGCAT-3'	3,563–3,592	Mutagenesis #
VWF_C1099A_Rv	30	5'-AATGGTGTCGCAGAA**GGC**GGCGCAGTCCCC-3'	3,533–3,562	Mutagenesis #
VWF_C1142A_Fw	32	5'-CGCTATAACAGCTGTGCACCTGCCTGTCAAGT-3'	3,683–3,714	Mutagenesis #
VWF_C1142A_Rv	30	5'-CCACTC**TGC**CTCATACCCGTTCTCCCGGAG-3'	3,653–3,682	Mutagenesis #
VWF_S2756A_Fw	30	5'-GACATCAACGATGTGCAGGACCAGTGCTCC-3'	8,537–8,566	Mutagenesis #
VWF_S2756A_Rv	30	5'-AATGGAGTACATGGCTTTG**GC**GGCACATTT-3'	8,507–8,536	Mutagenesis #

Nucleotide reference sequence NC_000012.12 in GRCh38.p13 (accessed on February 16th, 2021).

*: Sequence of primers for VWF exon 52 DNA sequencing. Positions correspond to those of the NCBI.

#: Sequence of primers for mutagenesis. Positions correspond to the number of coding DNA.